Published in final edited form as:
J Neurogenet. 2009 ; 23(1): 185–199. doi:10.1080/01677060802471726.

Role of *rut* adenylyl cyclase in the ensemble regulation of presynaptic terminal excitability: Reduced synaptic strength and precision in a *Drosophila* memory mutant

Atsushi Ueda and **Chun-Fang Wu**
Department of Biological Sciences, University of Iowa, Iowa City, IA 52242, USA

Abstract

Although modulation of presynaptic terminal excitability can profoundly affect transmission efficacy, how excitability along axonal terminal branches is regulated requires further investigations. We performed focal patch recording in *Drosophila* larval neuromuscular junctions (NMJs) to monitor activity of individual synaptic boutons along the presynaptic terminal. Analysis of the learning mutant *rutabaga* (*rut*) suggests a tight regulation of presynaptic terminal excitability by *rut* adenylyl cyclase (AC) that is responsible for Ca^{2+}/calmodulin-dependent cAMP synthesis. Focal excitatory junctional currents (ejcs) demonstrated that disrupted cAMP metabolism in *rut* mutant boutons leads to decreased transmitter release, coupled with temporal dispersion and amplitude fluctuation of ejcs during repetitive activity. Strikingly, *rut* motor terminals displayed greatly increased variability among corresponding terminal branches of identified NMJs in different preparations. However, boutons throughout single terminal branches were relatively uniform in either WT or *rut* mutant larvae. The use of electrotonic depolarization to directly evoke transmitter release from axonal terminals revealed that variability in neurotransmission originated from varying degrees of weakened excitability in *rut* terminals. Pharmacological treatments and axonal action potential recordings raised the possibility that defective *rut* AC resulted in reduced Ca^{2+} currents in the nerve terminal. Thus, our data indicate that *rut* AC not only affects transmitter release machinery but also plays a previously unsuspected role in local excitability control, both contributing to transmission level and precision along the entire axonal terminal.

Keywords

cAMP; synaptic plasticity; excitability and fidelity

INTRODUCTION

Neurotransmitter release is triggered by Ca^{2+} influx through voltage-dependent Ca^{2+} channels (Llinas et al., 1976; Zucker & Regehr 2002) and therefore presynaptic membrane excitability can profoundly affect transmission efficacy. Previous studies in both vertebrate and invertebrate preparations have suggested modifications of excitability at presynaptic terminals during activity-dependent processes, as inferred from soma recordings of action potential waveform, firing pattern, and associated Na^+ and K^+ currents (Byrne & Kandel 1996; Ganguly et al., 2000; Morozov et al., 2003). Since distinct ion channel subtypes are expressed in the soma and distal axonal synaptic terminals (Dodson & Forsythe 2004), these cellular compartments are likely to show different membrane properties. It is thus desirable to monitor

Corresponding Author, Dr. Chun-Fang Wu, Professor, Dept. of Biology, University of Iowa, Iowa City, IA 52242, USA, Fax number 319-335-1103, Telephone number: 319-335-1090, E-mail address: chun-fang-wu@uiowa.edu.

activities at synaptic sites directly in order to determine how local modifications of presynaptic excitability contribute to regulation of transmission efficacy.

The *Drosophila* larval neuromuscular preparation can be used for studying synaptic transmission at the neuromuscular junction (NMJ) of identifiable motor neurons (Jan & Jan, 1976; Wu et al., 1978; Johansen et al., 1989). Individual synaptic boutons along axonal terminals can be visualized under Nomarski optics to allow focal loose-patch recordings of local excitatory junctional currents (ejcs; Kurdyak et al., 1994; Renger et al., 2000) and imaging of activity-dependent accumulation of presynaptic Ca^{2+} (Macleod et al., 2002; Reiff et al., 2005; Ueda & Wu, 2006). Furthermore, activity-dependent plasticity of synaptic growth and function (Budnik et al., 1990; Zhong & Wu, 1991; Broadie et al., 1997; Kuromi & Kidokoro, 2000; Renger et al., 2000; Sigrist et al., 2003) has been described in detail, making this preparation an excellent model system for applying a wealth of genetic and molecular tools to analyze the regulatory mechanisms of synaptic efficacy.

The *Drosophila* memory mutant *rutabaga* (*rut*) is defective in Ca^{2+}/calmodulin-activated adenylyl cyclase (AC; Levin et al., 1992), resulting in decreased cAMP synthesis (Dudai & Zvi, 1984; Livingstone et al., 1984) and poor short-term memory (Tully & Quinn, 1985). It has been shown that mutant *rut* alleles are defective in transmitter release machinery, as evidenced by abnormal activity-dependent plasticity of synaptic transmission and ultrastructural modifications in synaptic boutons at larval NMJs (Zhong & Wu, 1991; Renger et al., 2000). In addition, altered Ca^{2+} and K^{+} currents have been demonstrated in nerve and muscle cells (Zhong & Wu 1993; Zhao & Wu, 1997; Bhattacharya et al., 1999). Therefore, it is important to examine how *rut* AC modulates local membrane excitability in presynaptic terminals and whether altered excitability and release machinery separately affect distinct aspects of synaptic transmission.

Our results from *rut* mutant larvae raised the possibility that disrupted cAMP metabolism decreased presynaptic membrane excitability, leading to poor fidelity in timing and amplitude of transmission, as well as striking variability in transmission levels among different motor terminals. A combination of electrical recording techniques revealed the separate roles of Ca^{2+} and Na^{+} channels in regulating presynaptic axonal and terminal electrical activities that control transmitter release. Our findings suggest a critical function of nerve terminal Ca^{2+} channels that has not been emphasized previously. These localized Ca^{2+} channels not only regulate synaptic output through Ca^{2+}-dependent release machineries but also take part in shaping local excitability patterns, which can influence the temporal and spatial aspects of transmitter release within the nerve terminal. Thus, cAMP-dependent modulation of Ca^{2+} channels can provide an effective means for adjusting transmission efficacy along the entire presynaptic terminal branch as a whole.

MATERIALS AND METHODS

Drosophila Stocks

The *Drosophila melanogaster* stocks used include a wild-type (WT) strain Canton-S and mutant alleles of *rutabaga*, rut^{1} and rut^{1084}. Use of two independent isolates of *rut* alleles helped exclude the possibility of phenotypic contributions from unidentified second-site genetic variations. A fly strain carrying UAS-GCaMP-9, a Ca^{2+}-responsive indicator for Ca^{2+} imaging (Wang et al., 2004), was a generous gift from Drs. Yalin Wang and Yi Zhong (Cold Spring Harbor Laboratory, Cold Spring Harbor, NY).

Larval Neuromuscular Preparations and Physiological Solutions

Post-feeding third instar larvae were used for physiological recordings. Physiological solution HL3 (Stewart et al., 1994) contains (in mM) 70 NaCl, 5 KCl, 20 $MgCl_2$, 10 $NaHCO_3$, 5 Trehalose, 115 Sucrose, and 5 HEPES, at pH 7.2. For experiments in Figure 5, Figure 6, Figure 8, and Figure 9, we used HL3.1 (Feng et al., 2004), which had the same ionic composition except for a reduced Mg^{2+} concentration (4 mM). The final Ca^{2+} concentration in recording saline is specified for each experiment. To evoke nerve action potentials and ejcs, the segmental nerves were severed from the ventral ganglion and stimulated with a suction electrode (10 μm inner diameter) through the cut end. Stimulation amplitude was adjusted to 2.0 to 2.5 times the threshold voltage to ensure a uniform stimulation condition among experiments. Stimulus duration was 0.1 or 0.5 ms. For experiments in Figure 3, Figure 4, Figure 7, and Figure 8, transmitter release evoked by direct electrotonic stimulation of the nerve terminals was examined when nerve action potentials was blocked with 3 μM TTX (Ganetzky & Wu, 1982). Depolarization (1 ms) was applied through the suction electrode near the nerve entry point in the proximity of motor terminals to increase the effectiveness of electrotonic stimulation. With increasing stimulus intensity, electrotonically evoked ejcs gradually increased in amplitude until a saturation level was reached. Throughout this study, we analyzed maximum levels of the electrotonically induced ejcs.

Focal Loose Patch-Clamp Recording

Extracellular focal recordings were performed as described previously (Renger et al., 2000). Briefly, fire-polished focal recording electrodes with inner diameter of 4–8 μm and outer diameter of 15–20 um were filled with HL3 saline and were placed over type I boutons on muscle 13. The pipette opening typically covered one type Ib boutons in both WT and *rut* preparations. Ejc signals were picked up with a loose-patch clamp amplifier (Patch Clamp 8510; Zeitz Instruments, Munich, Germany) and stored on VCR tapes with a Pulse Code Modulator (Neuro Data, model Neuro-Corder DR-384, New York, NY). All trials contained a calibration pulse to determine the electrode series and seal resistance in order to correct for current leakage at the pipette tip (Renger et al., 2000; Kurdyak et al., 1994). In rare occasions, biphasic currents have been observed in both WT and *rut*, and they were excluded from data analysis.

Intracellular ejp Recording and Extracellular Compound Action Potential Recording

Nerve-evoked and electrotonically induced neurotransmitter release were also recorded intracellularly from postsynaptic muscle fibres for experiments in Figure 8 and Figure 9. Intracellular glass microelectrodes were filled with 3 M KCl and had a series resistance of about 60 MΩ. Ejps were picked up with a direct current pre-amplifier (model M701 micro-probe system, WPI, Conn., USA). Compound action potentials were recorded extracellularly in the segmental nerve *en passant* in HL3.1 saline (Figure 5C and D; Wu et al., 1978;Ganetzky & Wu, 1982). Signals were picked up by a differential alternating-current amplifier (DAM-5A, WPI, Conn., USA).

Ca^{2+} Imaging of Nerve Terminals

Ca^{2+} imaging was performed as described previously (Ueda & Wu 2006) on an upright microscope (Eclipse E600FN, Nikon, Japan) equipped with a Xenon short arc light source (UXL-75XE, Ushio Inc, Japan). Fluorescence from the larval preparation was collected with a water immersion objective lens (40x, Fluoro, N.A. = 0.80) and captured with a CCD camera (SM256, Sci Measure Analytical Systems, Inc., Georgia, USA) and stored and analyzed, using a computer software system NEUROCCD-SM256 (Red Shirt Imaging, New Haven, CT). Targeted expression of the Ca^{2+}-sensitive fluorescent protein G-CaMP enabled monitoring Ca^{2+} dynamics in motor terminals. Motoneuron-specific Gal4 enhancer trap C164 was used

to drive expression of the transgene UAS-GCaMP-9 (Wang et al., 2004). GCaMP expression in type Ib or Is axon terminals varies among NMJs in different muscles. Our experiments used muscle 13, in which C164-driven GCaMP expression was not detected in type Ib terminals, but was in a satisfactory range for Ca^{2+} imaging in type Is terminals. To determine GCaMP fluorescence intensities of the presynaptic boutons embedded in the muscle fibre, background autofluorescence from the surrounding muscle regions was subtracted from the total reading of the bouton area. This procedure gave an estimate of the base line fluorescence measured before stimulation (F) for scaling the nerve activity-induced increase of fluorescent intensity (ΔF) of individual boutons. A stimulus frequency beyond 20 Hz was necessary to induce sufficient Ca^{2+} accumulation for reliable detection of GCaMP fluorescence changes (Reiff et al., 2005; Ueda & Wu 2006). The quantity $\Delta F/F$, indicating intracellular Ca^{2+} level changes, was determined from signals averaged over 4 to 9 pixels that cover one bouton area.

Statistical Analysis

Unless otherwise stated, student t-test was carried out with sequential Bonferroni adjustment for multiple comparisons. For CV of ejc amplitudes and SD of ejc peak time shown in Figure 4, t-test was carried out after logarithmic conversion of data to normal distribution.

RESULTS

Decreased Synaptic Output and Increased Transmission Variability among *rut* Motor Terminals

Motor axon terminals on each identified muscle fibres have stereotypic branching patterns and are visible under Nomarski optics in live larval neuromuscular preparations (Jan & Jan 1976; Atwood et al., 1993). We performed loose-patch focal recording mostly from the NMJ of muscle 13, which typically consists of a primary motor terminal of both type Ib and Is axons devoid of secondary branching (Johansen et al., 1989). Synaptic boutons at this identified NMJ are exposed on the upper muscle surface in the preparation, which allows satisfactory seal formation for effective measurements of ejcs from the boutons underneath the patch electrode (Figure 1A). Type Ib boutons are larger, providing a clear visual guide under Nomarski optics to position the electrode for monitoring synaptic transmission along the entire presynaptic terminal. Typically, we sampled two terminals per larva, among abdominal segment 3 to 5. Running in close parallel to the type Ib terminal is the type Is terminal, which contains smaller type Is boutons and traverses a longer distance (Figure 1A). We discarded a small portion of NMJs in which the type Ib and Is terminals were not closely associated. This condition was found more often only in certain mutant genotypes but was rarely encountered in *rut* and WT.

We selected the pipet size such that the pipet lumen and wall cover both type Ib and Is boutons in the two motor terminals. Under Nomarski optics, we did not find any indications of different sizes of either type Ib or Is boutons between WT and *rut*. Therefore, ejc responses from type Ib and Is boutons were collected jointly under this condition. However, type Ib and Is responses could be separately detected by manipulations of recording sites or stimulation conditions. When stimulating the severed end of the segmental nerve, the larger ejc response of the type Is boutons arrived first because of a faster propagation speed of action potentials in the type Is axon (Figure 1B, ○). The delayed arrival of type Ib ejc response was detected as a smaller hump following the peak of type Is ejc (Figure 1B, ●). The larger type Is component could also be observed in isolation when the recording site was moved distally beyond the type Ib ending (‘a’ in Figure 1A and B; cf. Kurdyak et al., 1994). Alternatively, the two components could be separated based on their different thresholds. By slowly increasing the stimulus intensity, type Is ejcs were first recruited until the type Ib component appeared at higher stimulus intensities (Figure 1C). These differential ejc properties are consistent with previous studies on focal ejcs collected from isolated type Ib and Is boutons in *Drosophila* larval NMJs (Kurdyak et al.,

1994), as well as from the homologous synaptic boutons in the crayfish (Atwood & Govind 1990). Therefore, in the analysis throughout this paper, we applied stimuli closer to the nerve terminals and recruited both type Ib and Is responses at higher stimulus intensities to avoid separation of the two components (Figure 1D).

Under this condition, one striking *rut* phenotype was a great reduction in ejc amplitudes (Figure 1E, 1.5 mM Ca^{2+} in HL3 saline). With the Ib and Is responses combined, a majority of recording sites (> 70 %) in *rut* NMJs produced ejcs smaller than 2nA, whereas ejcs greater than 2 nA were observed in a majority (> 80 %) of WT samples (Figure 1E, arrows). Significantly, the following experiment indicated reduced ejc sizes for both Is and Ib boutons in *rut*. When type Ib and Is ejc components were extracted from the peak and superimposing hump of the responses (cf. Figure 1B; with stimuli applied at a distant location of the nerve), the pooled result from a large number of recording sites indicated a clear reduction in both Ib and Is components in *rut* (Figure 1F).

Systematic sampling of the combined Is and Ib ejc responses along the nerve terminal on muscle 13 revealed that ejc amplitudes were rather uniform within individual terminals for both WT and *rut*. However, among *rut* motor terminals from different muscle 13 samples, ejc amplitudes were highly variable, as compared to WT ejcs (Figure 2A). As shown in Figure 1E, the focal ejc size of 2 nA served as a useful criterion to demarcate two synaptic output levels reflecting the presence of high- and low-output terminals (Figure 2A, filled and open symbols). Note that ejc amplitudes varied about two orders of magnitude among terminals in *rut* vs. about one order among those in WT. (SD of $\log\overline{ejc}$among terminals, estimated by one-way ANOVA, was 0.34 for WT and 0.46 for *rut*, $p < 0.001$, F-test.) However, variability in focal ejcs within individual terminals was much smaller than that between terminals for both *rut* and WT. (SD within branch was 0.17 for WT and 0.18 for *rut*, $p > 0.05$, F-test.) It should be noted that a greater variation of ejc amplitudes was also observed between motor terminals within individual *rut* preparations as compared to that in single WT larvae (data not shown).

The above analysis was also performed on axonal terminals of additional identified muscle fibres, including muscles 1, 2, 4, and 12. The results support the general conclusions that defective *rut* AC reduces focal ejc amplitudes and increases variation among different axonal terminals of a given identified muscle (data not shown).

In order to determine whether the output level of individual terminals reflects presynaptic or postsynaptic differences, we examined, in the absence of stimulation, miniature ejcs (mejcs) that represent responses to spontaneous quantal release of transmitter. Focal recordings of mejcs from either high- or low-output terminals in WT as well as in *rut* showed similar mejc amplitudes, indicating no obvious differences in postsynaptic response to quantal transmitter release (Figure 2B). The similarity in quantal size suggests that variation in branch-output levels reflects variable quantal content of the evoked ejcs (i.e., variable number of released synaptic vesicles per stimulus from presynaptic terminals), rather than postsynaptic differences in receptor densities or properties. Note that frequency of spontaneous mejcs varied considerably among recording sites in both WT and *rut* (Figure 2C). However, in WT larvae, high frequencies of spontaneous mejcs were found only in high-output, whereas in both low- and high-output *rut* terminals, sites of high-frequency spontaneous release were observed, suggesting a potential contribution from altered presynaptic release machinery by the *rut* mutation.

Transmitter Release Capability in Axonal Terminal Branches in the Absence of Na^+ Action Potential

Altered transmitter release can be caused by modifications in a sequence of events, from Na^+ action potential invasion in nerve terminal branches, to local membrane excitation

supporting Ca^{2+} influx within the branch, and finally to Ca^{2+}-dependent activation of vesicle release machinery for transmitter discharge. To pinpoint the disruptions caused by *rut* mutations, we first investigated the release mechanisms when Na^{+} action potential invasion was bypassed. After TTX paralysis, Na^{+} action potential-initiated depolarization was replaced by direct electrotonic stimulation (1-msec duration, comparable to that of axonal action potential, see Methods) to artificially depolarize the terminal branch, which produced focal ejcs similar in shape to nerve evoked ejcs (Figure 3A). At individual recording sites, maximum ejc amplitudes were obtained by adjusting stimulation intensity. Significantly, ejcs from low-output boutons increased drastically in size, sometimes beyond an order of magnitude, especially in *rut* low-output terminals (Figure 3B). However, ejcs from high-output terminals increased only about two times on average in both WT and *rut*. In consequence, the maximum ejc amplitude attainable from high- and low-output terminals was not significantly different (Figure 3B). The above results suggest that altered presynaptic nerve excitability rather than synaptic release capability of individual boutons is responsible for the more abundant low-output terminals in *rut*.

Increased Variability in Short-Term Synaptic Plasticity among *rut* Terminals

In addition to more variable output levels among different terminals (Figure 2A), *rut* presynaptic terminals were also less predictable in short-term plasticity of transmission in a paired pulse (PP) stimulation protocol (Figure 3A; 20-ms inter-pulse interval). We determined the degree of facilitation or depression at different boutons, as indicated by PP facilitation index $\left(\overline{\text{ejc2}}/\overline{\text{ejc1}} - 1\right)$. In WT, high-output terminals displayed only depression (●, negative PP Indices), but both depression and facilitation were common in low-output terminals (△). However, high-output, as well as low-output, terminals in *rut* showed both facilitation and depression (Figure 3C; nerve-evoked). In general, a trend toward facilitation was found in *rut* terminals, which displayed higher facilitation in low-output terminals and less depression in high-output terminals compared to WT ($p < 0.01$ and 0.05 for high- and low-output terminals, respectively, Wilcoxon rank test). Notably, the spread of PP index was greater in low-output terminals for both WT and *rut*. Thus, a greater population of low-output terminals in *rut* resulted in highly variable PP index ($p < 0.001$; F-test).

Further experimentation indicated that presynaptic nerve excitability was responsible for the large variation in short-term plasticity among terminals. Upon direct electrotonic stimulation of the same nerve terminals, the range of ejc size converged considerably (Figure 3B) coupled with a drastic reduction of the variation in PP index (Figure 3C). The PP indices became uniformly negative (indicating depression) in both WT and *rut* terminals, regardless of their initial nerve-evoked output levels.

Amplitude Fluctuation and Temporal Dispersion of Transmission in *rut*

In addition to more extreme variability in synaptic terminal output levels, we also found poor timing and amplitude instability in the *rut* transmitter release process (Figure 4, left panels). Conceivably, such defects can increase the noise level during signal processing and may contribute to poor learning performance in *rut* flies. We examined the possibility that altered excitability in *rut* motor terminals contributes to temporal dispersion, as well as amplitude fluctuation, of ejcs by direct electrotonic stimulation of the nerve terminal in the presence of TTX (Figure 4. right panels). Before TTX application, *rut* terminals showed greater ejc amplitude variability (Figure 4A) and asynchronous release causing broadened or multiple-peak ejcs (Figure 4C). Such differences were reflected by a larger coefficient of variation (CV) of ejc amplitude and SD of time to peak in both high- and low-output *rut* terminals (Figure 4B and D). Using electrotonic stimulation following TTX paralysis, however, we observed drastic decreases in both parameters of the action potential-independent ejc responses. Under this

condition, CV of *rut* ejc amplitudes was no longer different from that of WT (Figure 4B). These results indicate that altered presynaptic nerve excitability is a major source of the striking amplitude fluctuation of transmission in *rut*. Despite a significant improvement in timing after TTX application, temporal dispersion of *rut* ejcs nevertheless remained significantly broader than that of WT for both low- and highoutput terminals (Figure 4D). Therefore, a defective step in the transmitter release process, independent of nerve action potential, may contribute to dispersion of *rut* ejcs, consistent with a previous report of ultrastructural defects in *rut* presynaptic terminals (Renger et al., 2000).

Prior to the occurrence of focal ejcs, the loose patch pipet also detected a small action current deflection, indicating the arrival of axonal action potential, which could be eliminated by TTX (data not shown; cf. Katz & Miledi 1965a). We found that action potential arrival time did not vary within individual preparations, even in *rut* NMJs that displayed great dispersion of ejcs. Therefore, the temporal dispersion of *rut* ejcs (Figure 4C and D, left panels) was likely to originate from sources other than variability in axonal Na^+ action potential propagation speed.

TTX Sensitivity of Neuromuscular Transmission and Axonal Action Potential Propagation

To localize the source contributing to the striking variability in *rut* ejcs, we investigated the consequences of gradually suppressing the Na^+ action potential invasion process. During TTX application with stepwise concentration increments, we monitored changes in ejc size following partial or complete inhibition of Na^+ action potentials (Figure 5A). Ejcs from low-output boutons in both WT and *rut* were blocked at a TTX concentration as low as 0.03 μM. In contrast, ejcs from some WT high-output boutons were not blocked until a concentration of 1.0 μM was reached. In general, *rut* terminals displayed higher sensitivity to TTX blockade (Figure 5B).

To determine whether the increased TTX sensitivity of *rut* ejcs (Figure 5B) reflects alterations in axonal action potential prior to invasion of terminal branches, we recorded Na^+ action potential propagation en passant in the segmental nerve innervating the body wall muscles. Amplitude of compound action potentials was monitored while TTX was bath applied at increasing concentrations (Figure 5C and D). We found that the sensitivity of axonal action potentials to TTX blockade was highly variable in both WT and *rut* segmental nerves. Within the concentration range examined, some *rut* axons showed even higher resistance to TTX than WT axons (Figure 5D). This indicates that a weakened action potential mechanism along motor axons cannot count for the reduced output levels in *rut* terminals. Therefore, the observed increase in TTX sensitivity of *rut* ejcs (Figure 5B) reflects altered excitability mechanisms restricted to motor terminals.

Uniformity of Ca^{2+} Channel-Dependent Ca^{2+} Accumulation in Motor Terminal Branches

Altered Ca^{2+} channel activities can modify Ca^{2+} influx and activity-dependent intracellular Ca^{2+} dynamics. In order to visualize Ca^{2+} accumulation within WT and *rut* nerve terminals, we performed Ca^{2+} imaging on boutons along the terminus branch on muscle 13 with genetically encoded Ca^{2+}-sensitive green fluorescent protein, GCaMP. This Ca^{2+} sensor has been successfully applied in *Drosophila* sensory neurons (Wang et al., 2003; Wang et al., 2004) and motor terminals (Reiff et al., 2005, Ueda & Wu, 2006), although its slower kinetics does not allow detection of fast Ca^{2+} transients associated with transmitter release. The use of WT and *rut* strains expressing Ca^{2+}-sensitive GCaMP in motor axon terminals enabled measurements of fluorescence intensity to determine the distribution of Ca^{2+} accumulation at the single bouton resolution (Figure 6). Targeted expression of GCaMP was under the control of a motorneuron driver *C164 Gal4*. HL3.1 saline containing a reduced Ca^{2+} concentration (0.2 mM) was used to minimize technical problems introduced by muscle contraction.

Ca^{2+} accumulation within individual boutons was not visible upon single nerve stimuli, but became evident at high frequency (20 Hz) repetitive stimulation, consistent with previous studies, in which multiple spike activity is required to trigger fluorescence changes (Reiff et al., 2005; Ueda & Wu, 2006). We found relatively uniform amplitudes (Figure 6B) and kinetics (data not shown) of fluorescence changes at different sites along individual terminal branches in both WT and *rut*. This is consistent with the relatively uniform synaptic output levels within individual axon terminals (Figure 2A), presumably reflecting Ca^{2+} channel distribution along the terminal. Under this condition, GCaMP fluorescence changes ($\Delta F/F$) induced by high frequency stimulation were not significantly different between *rut* and WT terminals (Figure 6C, left). Nevertheless, differences in Ca^{2+} accumulation facilitated by 20-Hz repetitive stimulation became apparent when WT and *rut* terminals were challenged by a subthreshold dose of a Ca^{2+} channel blocker, Co^{2+} (Figure 6C, right). Interestingly, partial Ca^{2+} channel blockade produced not only greater reduction but also higher variability in $\Delta F/F$ among *rut* terminals (Figure 6D), representing an interesting parallel to the focal recording observation of more abundant low-output motor terminals that displayed greater variability in ejc amplitudes of an identified NMJ in *rut* (Figure 2A).

Increased Sensitivity of *rut* ejcs to Ca^{2+} Channel Blockade

Additional lines of evidence for weakened Ca^{2+} influx in *rut* terminals were obtained in pharmacological experiments with focal recordings of electrotonically evoked ejcs in the presence of TTX (Figure 7A). This approach removed influence from Na^{+}-dependent action potential invasion and produced ejcs of increased amplitudes and decreased variability, as shown above (cf. Figure 3 and Figure 4). In particular, such enhanced release facilitated quantification of drug effects in *rut* low-output terminals. We investigated the suppression of electrotonically evoked ejcs by a specific Ca^{2+} channel blocker, Cd^{2+}. The dose-dependent inhibition of ejcs under this condition provided an independent measure of the relative strength of Ca^{2+} influx in WT and *rut* terminals. As shown in Figure 7, ejcs were inhibited to a greater extent in *rut* at two different Cd^{2+} concentrations (2 and 6 μM). These observations support the idea that *rut* mutations alter Ca^{2+} channel density or properties (e.g., binding constant Kd, conductance, voltage dependence, etc.) and consequently affect transmitter release as well as local membrane excitability within motor terminals.

Altered Ca^{2+}-Dependent Excitability in *rut* Axon Terminal

One means to amplify the Ca^{2+}-supported excitability in presynaptic axon terminals after silencing Na^{+} spikes with TTX is to further remove the repolarization force by K^{+} channel blockers. Under this condition, we observed strikingly prolonged excitatory junctional potentials (ejps), with durations up to a few seconds, that reflected transmitter release triggered by sustained presynaptic Ca^{2+} action potentials (Figure 8). This is consistent with explosive, prolonged postsynaptic potentials first described in the squid giant synapse and the frog neuromuscular junction under similar conditions (Katz & Miledi, 1969ab).

We recorded intracellularly such prolonged ejps in response to direct electrotonic stimulation in the presence of TTX, 4-AP, TEA, and quinidine (Figure 8A; cf. Ganetzky & Wu, 1982, 1983). The experiments were performed with 0.1 mM Ca^{2+} in saline to minimize muscle contraction. These plateau potentials, both evoked by electrotonic stimulation and occurring spontaneously, represented prolonged transmitter release, rather than muscle Ca^{2+} spikes, because they were not overshooting and were not terminated by hyperpolarizing current injection in the muscle (data not shown). The role of presynaptic Ca^{2+} channels in generating such prolonged transmitter release was indicated by application of a low dose of the Ca^{2+} channel blocker, Co^{2+}, which reduced both amplitude and duration of plateau ejps (Figure 8A). The plateau ejps are unstable, nonlinear events, not triggered at every trial with identical electrotonic stimuli (arrowheads in Figure 8A), but nevertheless, provide quantifiable indices

for presynaptic excitability. The probability of success in triggering plateau ejps increased with increasing stimulus intensity until a maximum rate was reached, but once triggered, the amplitude and duration were independent of stimulus voltage. Our data demonstrate that the success rate of evoking plateau ejps was significantly reduced in *rut* (Figure 8B).

In addition, plateau ejps also occurred spontaneously at a low frequency, with amplitudes varying from a few milli-volts up to the size comparable to the evoked ones (Figure 8A; dots), presumably reflecting local excitation events due to instability of axon terminal membrane potential. We quantified these spontaneous events with amplitudes at least 20% of the evoked ones, which constitute a majority of spontaneous events in WT. The occurrence of such spontaneous plateau ejps was significantly reduced in *rut*, with an interval of minutes between events compared to tens of seconds in WT (Figure 8C).

The above results support the notion that in addition to Na^+ channels, Ca^{2+} channels, known to be abundant in presynaptic terminals, participate in regulation of local membrane depolarization. The interplay between Ca^{2+} and Na^+ channels in regulating nerve terminal excitability was further studied by simultaneous recordings of postsynaptic muscle ejps and motor axon action potentials. As previously described (Ganetzky & Wu, 1982, Ueda & Wu, 2006), this interaction is best demonstrated after suppression of nerve repolarization by K^+ channel blockers (4-AP and TEA, without adding TTX). With the contribution from axonal Na^+ channels, activation of terminal Ca^{2+} channels forms a positive feedback loop and this sustained interplay supports multiple firing and prolonged transmitter release. Under this condition, plateaued potentials occurred more regularly than those triggered by electrotonic stimulation following TTX blockade of Na^+ channels displayed in Figure 8. Consistently, single nerve stimuli evoked prolonged ejps coupled with axonal multiple firing (Figure 9, arrowheads). Furthermore, such axonal multiple firing and prolonged ejps also occurred spontaneously. As previously shown, following the initial action potential, the supernumerary spikes propagated antidromically from the terminal back to the soma (Ganetzky & Wu, 1982, Ueda & Wu, 2006).

These explosive plateaued potentials are highly non-linear regenerative events. Differences between *rut* and CS are more evident in the occurrence rather than amplitude or duration of the response (Figure 8). Further experiments using sub-threshold doses of Co^{2+} or Cd^{2+} for partial Ca^{2+} channel blockade (cf. Figure 7) will provide additional lines of evidence for reduced Ca^{2+} influx in *rut* NMJs. Taken together, the results of Figure 7–Figure 9 support a critical role of Ca^{2+} currents in local control of terminal excitability and suggest potential modulation of Ca^{2+} channels by *rut* AC for regulating the overall synaptic activity along the axonal terminal branch.

Discussion

Axonal Terminal Excitability and Synaptic Plasticity: Role of Ca^{2+} Channels

Among well-established mechanisms underlying learning and memory and other neural plasticity processes, postsynaptic receptor regulation has been extensively studied and documented (Malinow & Malenka, 2002). Although modulation of presynaptic membrane excitability has also been implicated in activity-dependent synaptic plasticity, direct examination of axon terminal excitability has been scarce. Our study presents evidence for modulation of terminal excitability by *rut* AC from direct monitoring of local activities along nerve terminals. It is known that presynaptic terminals are enriched with Ca^{2+} and K^+ channels (Dodson & Forsythe 2004; Evans & Zamponi, 2006). Indeed, mutations affecting different outward K^+ currents, including those mediated by *eag*, *Sh*, and *Shab* channels, have been shown to profoundly influence synaptic strength and activity-dependent plasticity at *Drosophila* larval NMJs (Jan et al., 1977; Ganetzky & Wu 1982; 1983; Stern & Ganetzky, 1989; Ueda & Wu,

2006). In this paper, our work demonstrates the important role of inward currents mediated by Ca^{2+} channels in nerve terminal excitability and plasticity. Although Ca^{2+} influx has long been identified as the source for triggering synaptic transmitter release (Katz & Miledi 1965b), our findings illustrate a less emphasized role of Ca^{2+} channel-supported excitability that determines the efficacy of invading Na^{+} action potentials in eliciting transmission throughout the axonal terminal.

Role of cAMP in Presynaptic Mechanisms

Our data demonstrate that *rut* mutations lead to a higher proportion of low-output terminals and increased sensitivity of transmitter release to Ca^{2+} channel blockers. These observations are consistent with the idea that *rut* mutations alter Ca^{2+} channel properties (e.g. changes in channel activation voltage or conductance) or down regulate Ca^{2+} channel expression. Ca^{2+} channels have been shown to be modulated by cAMP pathway in the neuronal soma of both vertebrates and invertebrates (Chad et al., 1987; Kits & Mansvelder 1996). In *Drosophila*, Ca^{2+} currents in larval muscles are decreased when the cAMP pathway is suppressed by mutations and drugs (Bhattacharya et al., 1999). Synaptic terminals of *rut* can support nearly WT-level transmitter release but require direct electrotonic stimulation to sustain sufficient Ca^{2+} influx, i.e., conversion of low output to high output terminal terminals (Figure 3), raising the possibility that Ca^{2+} channels in presynaptic terminals are also modulated by cAMP-dependent mechanisms.

Pharmacological and genetic evidence has established a role of the cAMP pathway in different forms of plastic behaviours, including spatial memory in mice (Martin et al., 2000), associative and non-associative conditioning in *Aplysia* (Bailey et al., 2004), and olfactory associative learning in *Drosophila* (Dudai et al., 1976; Tully & Quinn 1985). At the cellular level, cAMP has also been implicated in synaptic plasticity in vertebrate and invertebrate species. Protein-kinase A (PKA) and the associated downstream mechanisms underlie long-term synaptic facilitation in invertebrates (Kandel et al., 1987; Dixon & Atwood 1989) and long-term synaptic potentiation in mammalian hippocampal and cortical neurons (Tong et al., 1996; Abel et al., 1997). In *Drosophila* neuromuscular junctions, mutations that disrupt cAMP metabolism, such as *dunce* (phosphodiesterase; Byers et al., 1981) and *rut*, have also been shown to alter synaptic vesicle pool dynamics (Kuromi & Kidokoro 2000), synaptic vesicle distribution, electron-dense areas (Renger et al., 2000), and post-tetanic potentiation of transmission (Zhong & Wu 1991). Our results extend the important role of cAMP-dependent modulation in synaptic plasticity to Ca^{2+} channel-dependent presynaptic terminal excitability.

Notably, among multiple *rut* alleles examined, rut^{1} displayed the most striking phenotype whereas rut^{1084} (Figure 8) and rut^{2} (data not shown) had much less extreme defects. This is consistent with the previous report that rut^{1} is more effective than other alleles in suppressing synaptic terminal overgrowth caused by hyperexcitable K^{+} channel mutations (Zhong et al., 1992). The rut^{1} mutation is special in that it eliminates Ca^{2+}/Calmodulin-dependent activation of AC activity (Dudai & Zvi 1984;Livingston et al., 1984) and thus disrupts synaptic plasticity conferred by activity-dependent Ca^{2+} accumulation in nerve terminals.

Global vs Local Regulatory Mechanisms of Synaptic Plasticity

The characteristic phenotypes of *rut* axon terminals demonstrate the important role of terminal excitability in regulating the stability and timing of synaptic transmission. We observed increased variability of synaptic transmission at individual boutons in terms of amplitude fluctuation and temporal dispersion of ejcs during repetitive activity (Figure 4; cf. Renger et al., 2000). More importantly, an even greater variability was found among *rut* axon terminals in different NMJs, with ejc amplitudes spanning about two orders of magnitude (Figure 2). When Ca^{2+} influx was activated by electrotonic stimulation in place of intrinsic excitability

mechanisms, amplitude fluctuation within individual boutons (Figure 4A and B) and variation in ejc amplitudes among different boutons (Figure 3B) was drastically reduced in *rut* terminals. In contrast, a significant portion of temporal dispersion of ejcs still remained (Figure 4C and D), implying that, in addition to axon terminal excitability, *rut* also affects the synaptic release machinery. This is consistent with the reported ultrastructural changes of synaptic structure and vesicular distribution in *rut* boutons (Renger et al., 2000).

Presumably, reduced terminal excitability due to disrupted cAMP regulation can confine the operational range and limit synaptic transmission to near threshold levels, making the system more prone to noise interference. This condition was seen in many low-output branches and resembles the highly variable quantal fluctuations of synaptic transmission observed at low external Ca^{2+} levels (Fatt and Katz, 1952). Thus direct electrotonic depolarization could extend the operational range, increasing amplitude and reducing variability of transmission (Figure 3 and Figure 4).

It should be emphasized that ejc amplitudes at different recording sites were relatively uniform along individual axon terminals, varying only about two fold within a terminal for both WT and *rut*, regardless of the output levels (Figure2A). Previous Ca^{2+} imaging studies have also examined variations in Ca^{2+} dynamics along individual motor terminals in *Drosophila* larvae by using Ca^{2+} sensitive probes expressed in pre- (Lnenicka et al., 2006) and post- (Guerrero et al., 2005) synaptic sites. However, the variability within individual terminals from these reports is far less than the focal ejcs among different *rut* motor terminals described here (Figure 2A).

Our work provides an interesting contrast between the roles of membrane excitability versus vesicle release machinery in the functioning of the presynaptic terminal as a whole. Current research into the mechanisms of synaptic plasticity emphasizes coordinated modulation of the presynaptic transmitter release (Leender & Sheng 2005) and the postsynaptic receptor response (Malinow & Malenka, 2002). Such mechanisms enhance local regulations of synaptic strength for pairing of specific pre- and postsynaptic partners, as well as association of two neighbouring inputs (Bi & Poo 2001). However, a great range of synaptic output levels varying among individual axon terminals observed in *rut* mutants raises the possibility of a different form of regulation, i.e. adjustment of transmission efficacy along the entire presynaptic terminal branch as a whole by cAMP-dependent modulatory mechanisms. In the case of CNS neurons, their axons are connected to numerous targets cells that may thus affect ensembles of postsynaptic neurons of various functional categories. Such global control of branch excitability can maximize the effect of a single neuron output to influence a diversity of postsynaptic components in the circuits underlying different functional tasks.

REFERENCES

Abel T, Nguyen PV, Barad M, Deuel TAS, Kandel ER. Genetic demonstration of a role for PKA in the late phase of LTP and in hippocampus-based long-term memory. Cell 1997;88:615–626. [PubMed: 9054501]

Atwood HL, Govind CK. Activity-dependent and age-dependent recruitment and regulation of synapses in identified crustacean neurons. J. exp. Biol 1990;153:105–127.

Atwood HL, Govind CK, Wu CF. Differential ultrastructure of synaptic terminals on ventral longitudinal abdominal muscles in *Drosophila* larvae. J. Neurobiol 1993;24:1008–1024. [PubMed: 8409966]

Bailey CH, Kandel ER, Si K. The persistence of long-term memory: a molecular approach to self-sustaining changes in learning-induced synaptic growth. Neuron 2004;44:49–57. [PubMed: 15450159]

Bhattacharya A, Gu GG, Singh S. Modulation of dihydropyridine-sensitive calcium channels in *Drosophila* by a cAMP-mediated pathway. J. Neurobiol 1999;39:491–500. [PubMed: 10380071]

Bi G, Poo M. Synaptic modification by correlated activity: Hebb's postulate revisited. Annu. Rev. Neuosci 2001;24:139–166.

Broadie K, Rushton E, Skoulakis EMC, Davis RL. Leonardo, a *Drosophila* 14-3-3 protein involved in learning, regulates presynaptic function. Neuron 1997;19:391–402. [PubMed: 9292728]

Budnik V, Zhong Y, Wu CF. Morphological plasticity of motor axons in *Drosophila* mutants with altered excitability. J. Neurosci 1990;10:3754–3768. [PubMed: 1700086]

Byers D, Davis RL, Kiger JA Jr. Defects in cyclic AMP phosphodiesterase due to the dunce mutation of learning in Drosophila melanogaster. Nature 1981;289:79–81. [PubMed: 6256649]

Byrne JH, Kandel ER. Presynaptic facilitation revisited: State and time dependence. J. Neurosci 1996;6:425–435. [PubMed: 8551327]

Chad J, Kalman D, Armstrong D. The role of cyclic AMP-dependent phosphorylation in the maintenance and modulation of voltage-activated calcium channels. Soc. Gen. Physiol. Ser 1987;42:167–186. [PubMed: 2850609]

Dixon D, Atwood HL. Adenylate cyclase system is essential for long-term facilitation at the crayfish neuromuscular junction. J. Neurosci 1989;9:4246–4253. [PubMed: 2480401]

Dudai Y, Jan YN, Byers D, Quinn WG, Benzer S. dunce, a mutant of *Drosophila* deficient in learning. Proc. Natl. Acad. Sci 1976;73:1684–1688. [PubMed: 818641]

Dudai Y, Zvi S. Adenylate cyclase in the *Drosophila* memory mutant rutabaga displays an altered Ca^{2+} sensitivity. Neurosci. Lett 1984;47:119–124. [PubMed: 6462535]

Dodson PD, Forsythe ID. Presynaptic K^+ channel: electrifying regulators of synaptic terminal excitability. Trends. Neurosci 2004;27:210–217. [PubMed: 15046880]

Evans RR, Zamponi GW. Presynaptic Ca^{2+} channels – integration centers for neuronal signaling pathways. Trends. Neurosci 2006;29:617–624. [PubMed: 16942804]

Fat P, Katz B. Spontaneous subthreshold activity at motor nerve endings. J. Physiol 1952;117:109–128. [PubMed: 14946732]

Feng Y, Ueda A, Wu CF. A modified minimal haemolymph-like solution, HL3.1, for physiological recordings at Drosophila larval neuromuscular junctions. J. Neurogenet 2004;18:377–402. [PubMed: 15763995]

Ganetzky B, Wu CF. *Drosophila* mutants with opposing effects on nerve excitability: Genetic and spatial interactions in repetitive firing. J. Neurophysiol 1982;47:501–514. [PubMed: 6279790]

Ganetzky B, Wu CF. Neurogenetic analysis of potassium currents in *Drosophila*: Synergistic effects on neuromuscular transmission in double mutants. J. Neurogenet 1983;1:17–28. [PubMed: 6100303]

Ganguly K, Kiss L, Poo M. Enhancement of presynaptic neuronal excitability by correlated presynaptic and postsynaptic spiking. Nat. Neurosci 2000;3:1018–1026. [PubMed: 11017175]

Guerrero G, Rieff DF, Agarwal G, Ball RW, Borst A, Goodman CS, Isacoff EY. Heterogeneity in synaptic transmission along a *Drosophila* larval motor axon. Nat. Neurosci 2005;8:1188–1196. [PubMed: 16116446]

Jan LY, Jan YN. Properties of the larval neuromuscular junction of *Drosophila melanogaster*. J. Physiol 1976;262:215–236. [PubMed: 186587]

Jan YN, Jan LY, Dennis MJ. Two mutations of synaptic transmission in *Drosophila*. Proc. R. Soc. Lond. B. Biol. Sci 1977;198:87–108. [PubMed: 20636]

Johansen J, Halpern ME, Johansen KM, Keshishian H. Stereotypic morphology of glutamatergic synapses on identified muscle cells of *Drosophila* larvae. J. Neurosci 1989;9:710–725. [PubMed: 2563766]

Kandel, ER.; Klein, M.; Hochner, B.; Shuster, M.; Siegelbaum, SA.; Hawkins, RD.; Glanzman, DL.; Castellucci, VF.; Abrams, TW. Synaptic modulation and learning: New insights into synaptic transmission from the study of behavior. In: Edelman, CM.; Gall, WE.; Cowan, WM., editors. Synaptic Function. New York: John Wiley & Sons, Inc; 1987. p. 471-518.

Katz B, Miledi R. Propagation of electric activity in motor nerve terminals. Proc. R. Soc. Lond. B. Biol. Sci 1965a;161:453–482. [PubMed: 14278408]

Katz B, Miledi R. Effect of calcium on acetylcholine release from motor nerve terminals. Proc. R. Soc. Lond. B. Biol. Sci 1965b;161:496–503. [PubMed: 14278410]

Katz B, Miledi R. Tetrodotoxin-resistant electric activity in presynaptic terminals. J. Physiol 1969a; 203:459–487. [PubMed: 4307710]

Katz B, Miledi R. Spontaneous and evoked activity of motor nerve endings in calcium ringer. J. Physiol 1969b;203:689–706. [PubMed: 4318717]

Kits KS, Mansvelder HD. Voltage gated calcium channels in molluscs: classification, Ca^{2+} dependent inactivation, modulation and functional roles. Invert. Neurosci 1996;2:9–34. [PubMed: 9372153]

Kurdyak P, Atwood HL, Stewart BA, Wu CF. Differential physiology and morphology of motor axons to ventral longitudinal muscles in Larval *Drosophila*. J. Comp. Neurol 1994;350:463–472. [PubMed: 7884051]

Kuromi H, Kidokoro Y. Tetanic stimulation recruits vesicles from reserve pool via a cAMP-mediated process in *Drosophila* synapses. Neuron 2000;27:133–143. [PubMed: 10939337]

Leenders AG, Sheng ZH. Modulation of neurotransmitter release by the second messenger-activated protein kinase: Implications for presynaptic plasticity. Pharmacol. Ther 2005;105:69–84. [PubMed: 15626456]

Levin LR, Han PL, Hwang PM, Feinstein PG, Davis RL, Reed RR. The Drosophila learning and memory gene *rutabaga* encodes a Ca^{2+} / calmodulin-responsive adenylyl cyclase. Cell 1992;68:479–489. [PubMed: 1739965]

Livingstone MS, Sziber PP, Quinn WG. Loss of calcium / calmodulin responsiveness in adenylate cyclase of *rutabaga*, a Drosophila learning mutant. Cell 1984;37:205–215. [PubMed: 6327051]

Llinas R, Steinberg I, Walton K. Presynaptic calcium currents and their relation to synaptic transmission: Voltage clamp study in squid giant synapse and theoretical model for the calcium gate. Proc. Natl. Acad. Sci. U S A 1976;73:2918–2922. [PubMed: 183215]

Lnenicka GA, Grizzaffi J, Lee B, Rumpal N. Ca^{2+} dynamics along identified synaptic terminals in *Drosophila* larvae. J. Neurosci 2006;26:12283–12293. [PubMed: 17122054]

Macleod GT, Hegstrom-Wojtowicz M, Charlton MP, Atwood HL. Fast calcium signals in *Drosophila* motor terminals. J. Neurophysiol 2002;88:2659–2663. [PubMed: 12424301]

Malinow R, Malenka RC. AMPA receptor trafficking and synaptic plasticity. Annu. Rev. Neurosci 2002;25:103–126. [PubMed: 12052905]

Martin SJ, Grimwood PD, Morris GM. Synaptic plasticity and memory: An evaluation of the hypothesis. Annu. Rev. Neurosci 2000;23:649–711. [PubMed: 10845078]

Morozov A, Muzzio IA, Bourtchouladze R, Van-Strien N, Lapidus K, Yin DQ, Winder DG, Adams JP, Sweatt JD, Kandel ER. Rap1 couples cAMP signaling to a distinct pool of p42/44 MAPK regulating excitability, synaptic plasticity, learning, and memory. Neuron 2003;39:309–325. [PubMed: 12873387]

Reiff DF, Ihring A, Guerrero G, Isacoff EY, Joesch M, Nakai J, Borst A. In vivo performance of genetically encoded indicators of neural activity in flies. J. Neurosci 2005;25:4766–4778. [PubMed: 15888652]

Renger JJ, Ueda A, Atwood HL, Govind CK, Wu CF. Role of cAMP cascade in synaptic stability and plasticity: Ultrastructural and physiological analysis of individual synaptic boutons in *Drosophila* memory mutants. J. Neurosci 2000;20:3980–3992. [PubMed: 10818133]

Sigrist SJ, Reiff DF, Thiel PR, Stenert JR, Schuster CM. Experience-dependent strengthening of *Drosophila* neuromuscular junctions. J. Neurosci 2003;23:6546–6556. [PubMed: 12878696]

Stern M, Ganetzky B. Altered synaptic transmission in *Drosophila*-Hyperkinetic mutants. J. Neurogenet 1989;5:215–228. [PubMed: 2553904]

Stewart BA, Atwood HL, Renger JJ, Wang J, Wu CF. Improved stability of Drosophila larval neuromuscular preparations in hemolymph-like physiological solutions. J. Comp. Physiol. A 1994;175:179–191. [PubMed: 8071894]

Tong G, Malenka RC, Nicoll RA. Long-term potentiation in cultures of single hippocampal granule cells: A presynaptic form of plasticity. Neuron 1996;16:1147–1157. [PubMed: 8663991]

Tully T, Quinn WG. Classical conditioning and retention in normal and mutant *Drosophila melanogaster*. J. Comp. Physiol. A 1985;157:263–277. [PubMed: 3939242]

Ueda A, Wu CF. Distinct frequency-dependent regulation of nerve terminal excitability and synaptic transmission by I_A and I_K potassium channels revealed by *Drosophila Shaker* and *Shab* mutations. J. Neurosci 2006;26:6238–6248. [PubMed: 16763031]

Wang JW, Wong AM, Flores J, Vosshall LB, Axel R. Two-photon calcium imaging reveals an odor-evoked map of activity in the fly brain. Cell 2003;112:271–282. [PubMed: 12553914]

Wang Y, Guo HF, Pologruto TA, Hannan F, Hakker I, Svoboda K, Zhong Y. Stereotyped odor-evoked activity in the mushroom body of *Drosophila* revealed by green fluorescent protein-based Ca^{2+} imaging. J. Neurosci 2004;24:6507–6514. [PubMed: 15269261]

Wu CF, Ganetzky B, Jan LY, Jan YN, Benzer S. A *Drosophila* mutant with a temperature-sensitive block in nerve conduction. Proc. Natl. Acad. Sci. U S A 1978;75:4047–4051. [PubMed: 211514]

Zhao ML, Wu CF. Alterations in frequency coding and activity dependence of excitability in cultured neurons of *Drosophila* memory mutants. J. Neurosci 1997;17:2187–2199. [PubMed: 9045743]

Zhong Y, Wu CF. Altered synaptic plasticity in *Drosophila* memory mutants with a defective cyclic AMP cascade. Science 1991;251:198–201. [PubMed: 1670967]

Zhong Y, Budnik V, Wu CF. Synaptic plasticity in *Drosophila* memory and hyperexcitable mutants: Role of cAMP cascade. J. Neurosci 1992;12:644–651. [PubMed: 1371316]

Zhong Y, Wu CF. Differential modulation of potassium currents by cAMP and its long-term and short-term effects: *dunce* and *rutabaga* mutants of *Drosophila*. J. Neurogenet 1993;9:15–27. [PubMed: 8295075]

Zucker RS, Regehr WG. Short-term synaptic plasticity. Annu. Rev. Physiol 2002;64:355–405. [PubMed: 11826273]

ACKNOWLEDGMENTS

We thank Drs. Yalin Wang, and Yi Zhong for providing a fly stock carrying UAS-GCaMP. We also thank Dr. Wei-Dong Yao for helpful discussions and comments. This work was supported by NIH grants NS26528 and HD18577.

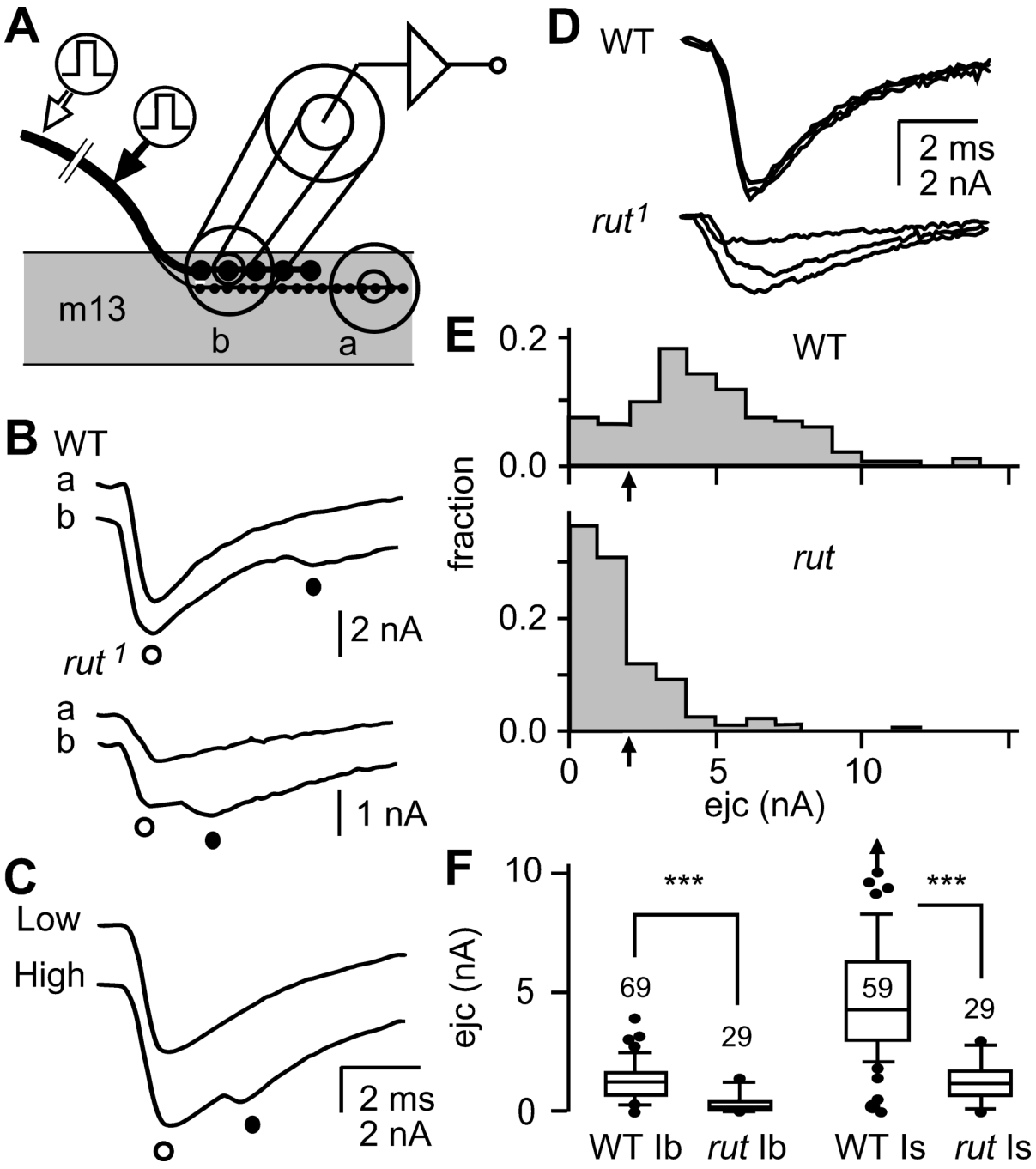

Figure 1.

Focal loose patch-clamp recordings of excitatory junctional currents (ejcs) from WT and *rut* nerve terminals at larval neuromuscular junctions (NMJs). **A**. Configuration of loose patch-clamp recording of ejcs. A fire-polished micropipette was placed over the synaptic boutons to record focal ejcs evoked by nerve stimulation. Most recordings were performed on muscle 13 where type Ib and Is terminals run closely and the recording pipet covered both types of boutons (site 'b'). Typically, type Is boutons traverse longer distance and type Is boutons could be recorded in isolation near the distal end of the terminal (site 'a'). **B**. Ejc components from type Is (○) and Ib (●) synaptic boutons. When stimulated at a distant site from the NMJ (open arrow in A, see text), ejcs with two peaks were recorded at site 'b' but a single peak at site 'a',

indicating that the 1st and 2nd peaks correspond to responses from type Is and Ib boutons, respectively. **C**. Separation of ejcs from type Ib and Is boutons at different stimulation intensities. The threshold of type Is axon was typically lower than that of type Ib axon and ejcs with two peaks appeared at site 'b' only at a higher stimulus intensity. **D**. Single-peak ejcs containing both type Ib and Is components were obtained when stimulation was applied closer to the nerve terminal (filled arrow in A). The shorter propagation distance did not significantly segregate the arrival time of action potential in type Is and Ib axons and the two ejc components completely overlapped. Superimposed traces demonstrate that *rut* ejcs were smaller and more variable under the same recording conditions. **E**. Amplitude distribution of focal ejcs in WT and *rut*. More than half of recording sites in *rut* NMJs produced ejcs smaller than 2 nA while the majority in WT yielded ejcs greater than 2 nA. In this study, the ejc size of 2 nA (arrow) was used to separate two distinct groups of axon terminals that exhibit high- and low-output transmission levels (see Figure 2A). N = 175 for WT and 130 for *rut*. **F**. Box plots comparing ejc amplitudes from type Ib and Is terminals between WT and *rut*. Arrow indicates an outlier beyond the scale. Numbers of recording sites were indicated. ***, $p < 0.001$; Mann-Whitney rank test with sequential Bonferroni adjustment.

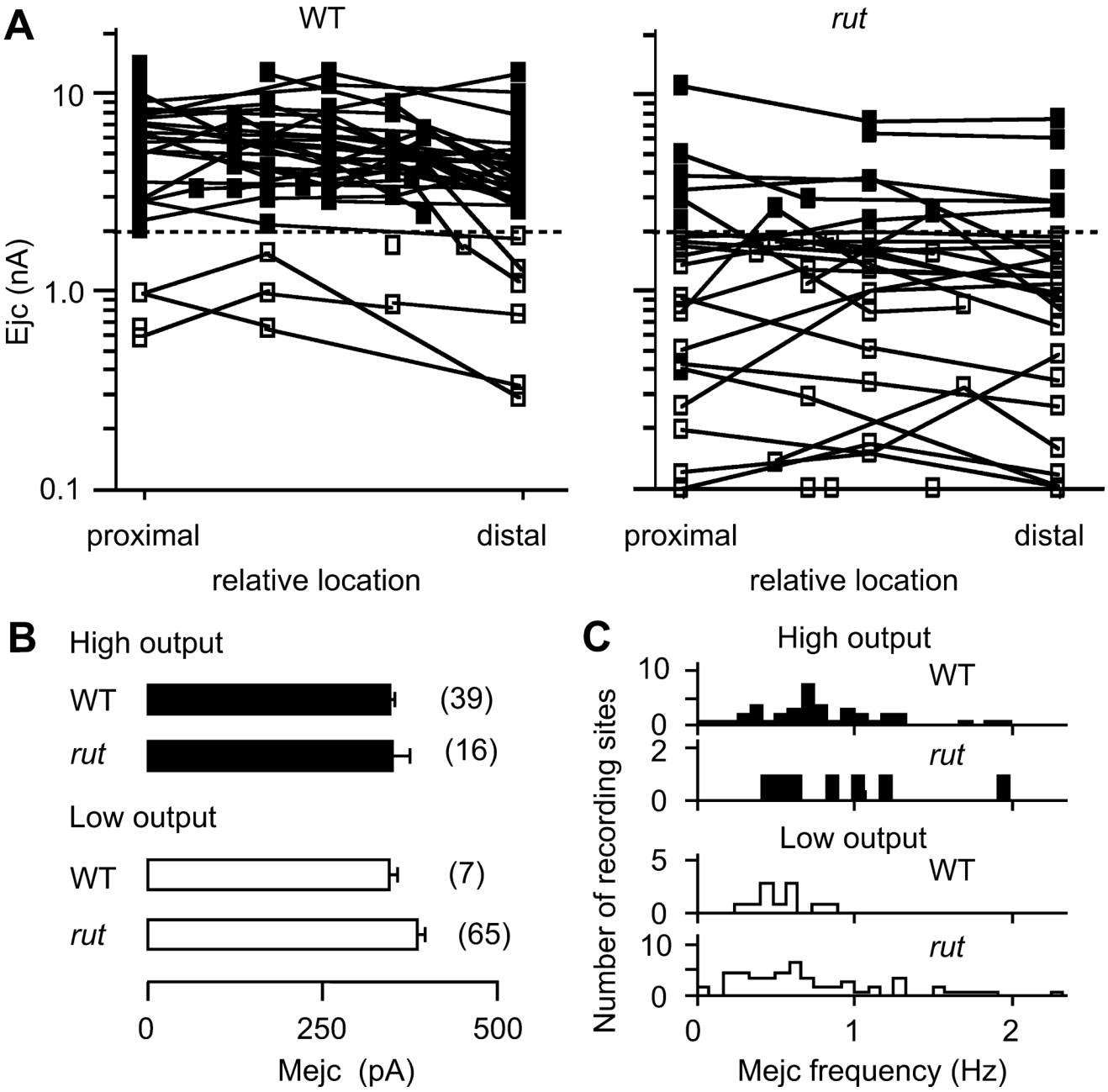

Figure 2.

Reduced synaptic output levels and increased variability among *rut* motor terminals. **A**. Highly variable synaptic output levels among *rut* terminals. The symbols represent the relative positions of recording sites along the type Ib terminal. Recording sites along individual high- and low-output terminals (with ejc amplitudes above and below 2 nA, separated by the dashed line) are represented by ■ and □, respectively, and are connected with line segments. **B**. No significant differences in spontaneous miniature ejc (mejc) amplitudes between high- (filled bar) and low-output (open bar) terminals and between WT and *rut*. Mean and SEM from the number of recording sites are indicated. **C**. Distributions of the rate of spontaneous mejcs. Note that for low-output terminals, mejcs were rare in WT but more frequent in *rut* ($p < 0.02$; t-test).

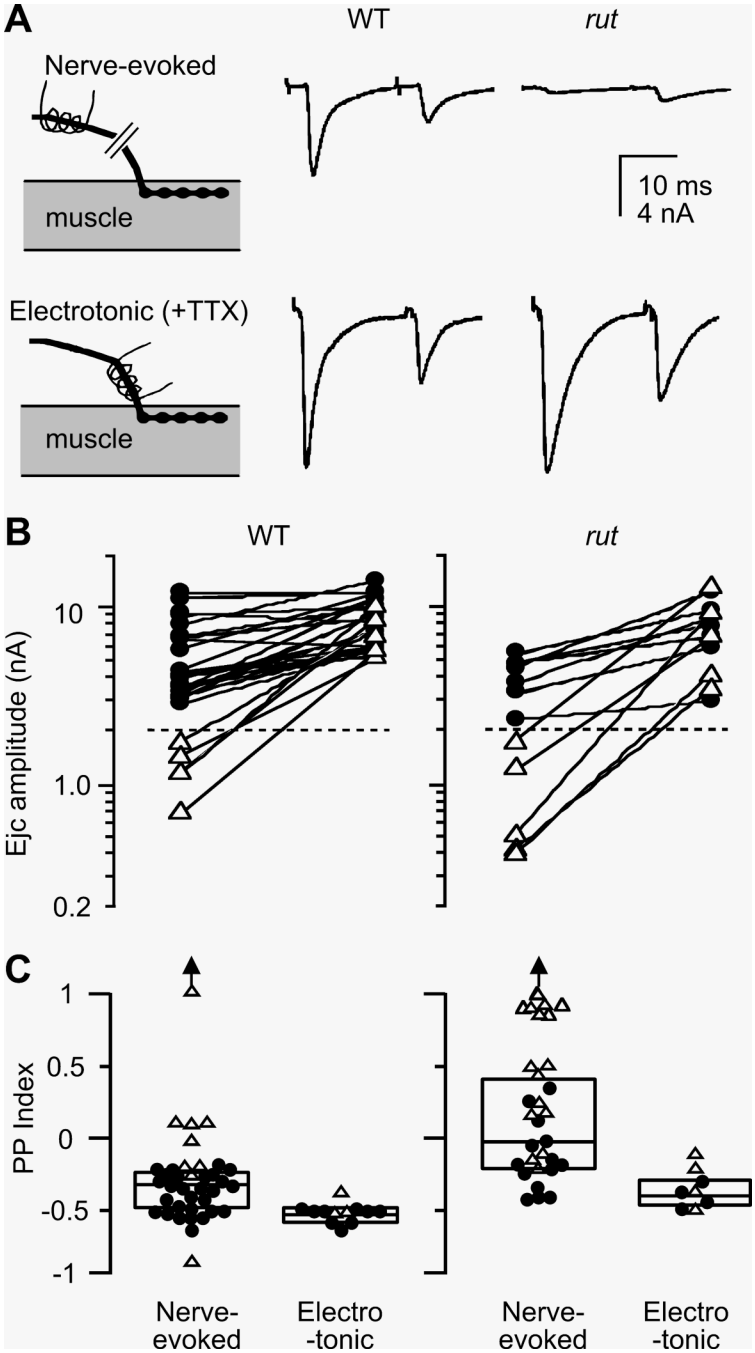

Figure 3.

Decreased synaptic variability by direct electrotonic stimulation of the nerve terminal. **A**. Focal ejcs evoked by nerve stimulation (upper panels) and by electrotonic stimulation of the terminal in the presence of 3 μM TTX (lower panels). In *rut* terminals, nerve-evoked ejcs were smaller and displayed paired pulse (PP) facilitation. When action potential invasion was by-passed by direct activation of release with electrotonic stimulation of the nerve terminal, greatly increased ejc size and PP depression was observed. In comparison, WT boutons displayed larger ejcs and PP depression. Traces represent averages of 4 – 8 trials. **B**. Release capability of boutons in high- and low-output terminals revealed by electrotonic stimulation. Ejcs evoked by nerve stimulation and by electrotonic stimulation from the same boutons are connected. Note that in

both WT and *rut*, release from low-output terminals became similar to that from high-output terminals when electrotonically stimulated. **C**. Decreased variability in facilitation/depression by electrotonic stimulation. Boutons in *rut* displayed a wideranging PP index $\left(\overline{\text{ejc}}_2/\overline{\text{ejc}}_1 - 1\right)$, from facilitation to depression, which became uniformly depression upon electrotonic stimulation. In contrast, WT boutons were more uniform and displayed mostly depression. The variability of PP index in WT was also decreased by electrotonic stimulation. ● and △ represent data from boutons in high- and low-output terminals, respectively (separated by dashed lines in panel B). Outliers beyond the scale are indicated by an arrow.

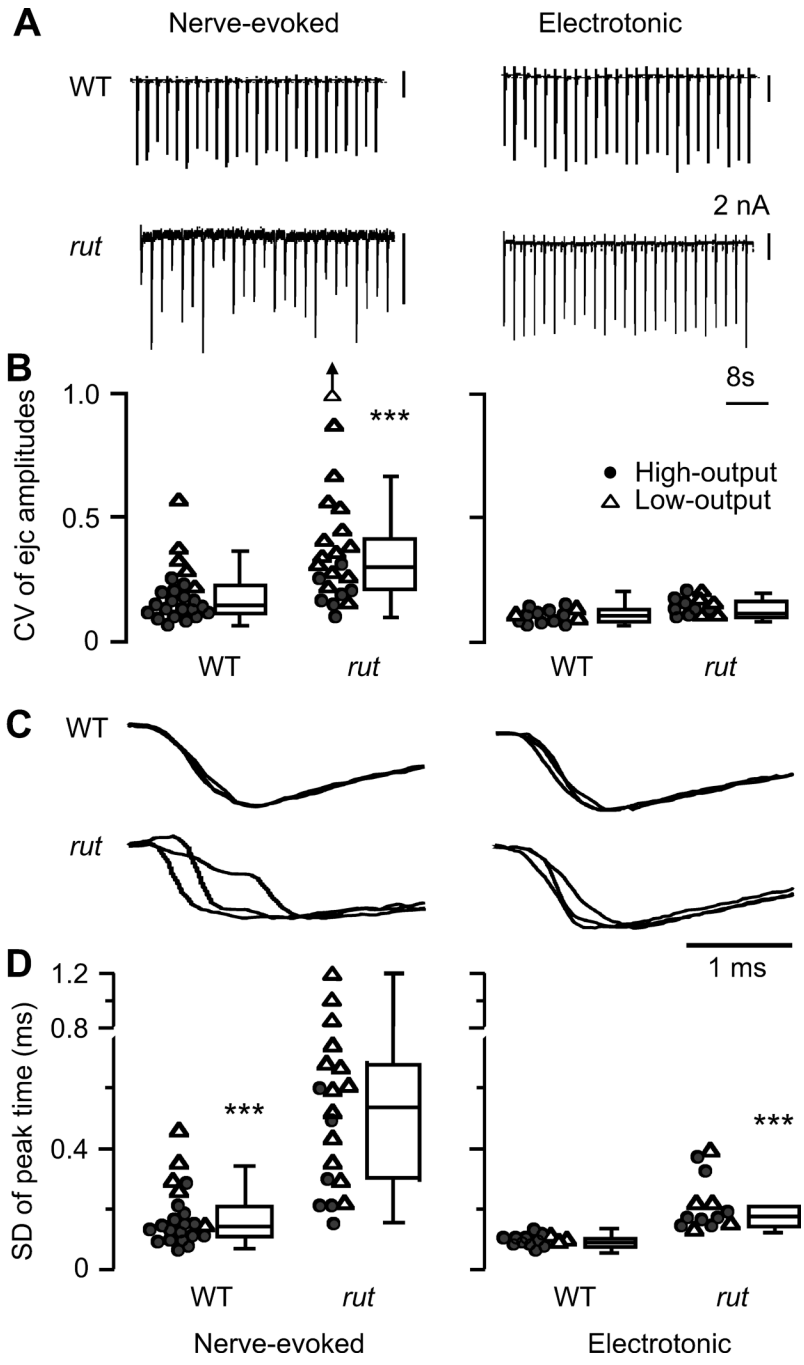

Figure 4.

Improved amplitude stability and temporal precision of transmission in *rut* terminals by electrotonic stimulation. **A**. Stability of ejc amplitude during repetitive nerve and electorotonic stimulation in WT and *rut* terminals. **B**. Coefficient of variation (CV) of ejc amplitude, showing greater instability of *rut* ejcs than WT ejcs ($p < 0.001$, ttest). In addition, CVs for low-output terminals (△) were higher than high-output terminals (●) in both WT and *rut* ($p < 0.001$). Such differences were absent in electrotonically induced ejcs ($p > 0.05$), indicating a role of TTX-sensitive action potential invasion in transmission stability. An outlier beyond the scale is indicated by an arrow. **C**. Representative traces showing altered temporal precision of

transmitter release during repetitive stimulation in *rut*. Ejcs in three successive trials were normalized for time course comparison. **D**. SD of time to ejc peak as an indicator for temporal precision of release. SD of nerve evoked ejcs is bigger in *rut* than that in WT ($p < 0.001$, t-test). Note that temporal precision was improved by direct electrotonic activation of release, indicating a role of nerve terminal excitability. However, even with electrotonic stimulation, some asynchronicity persisted in *rut* ejcs (WT < *rut*, $p < 0.001$, t-test), suggesting an impaired vesicle release mechanism. Data from all high- and low-output samples examined are presented in box plots. In scatter plots, ● and △ represents data from high- and low-output terminals, respectively. For clarity, some of the scatter plots include representative data points selected according to the rank order: one out of every 5 data points for CV of both WT and *rut* nerve-evoked ejcs; every 4 and 2 for SD of nerve-evoked WT and *rut* ejcs; every 2 for electrotonically induced WT ejcs.

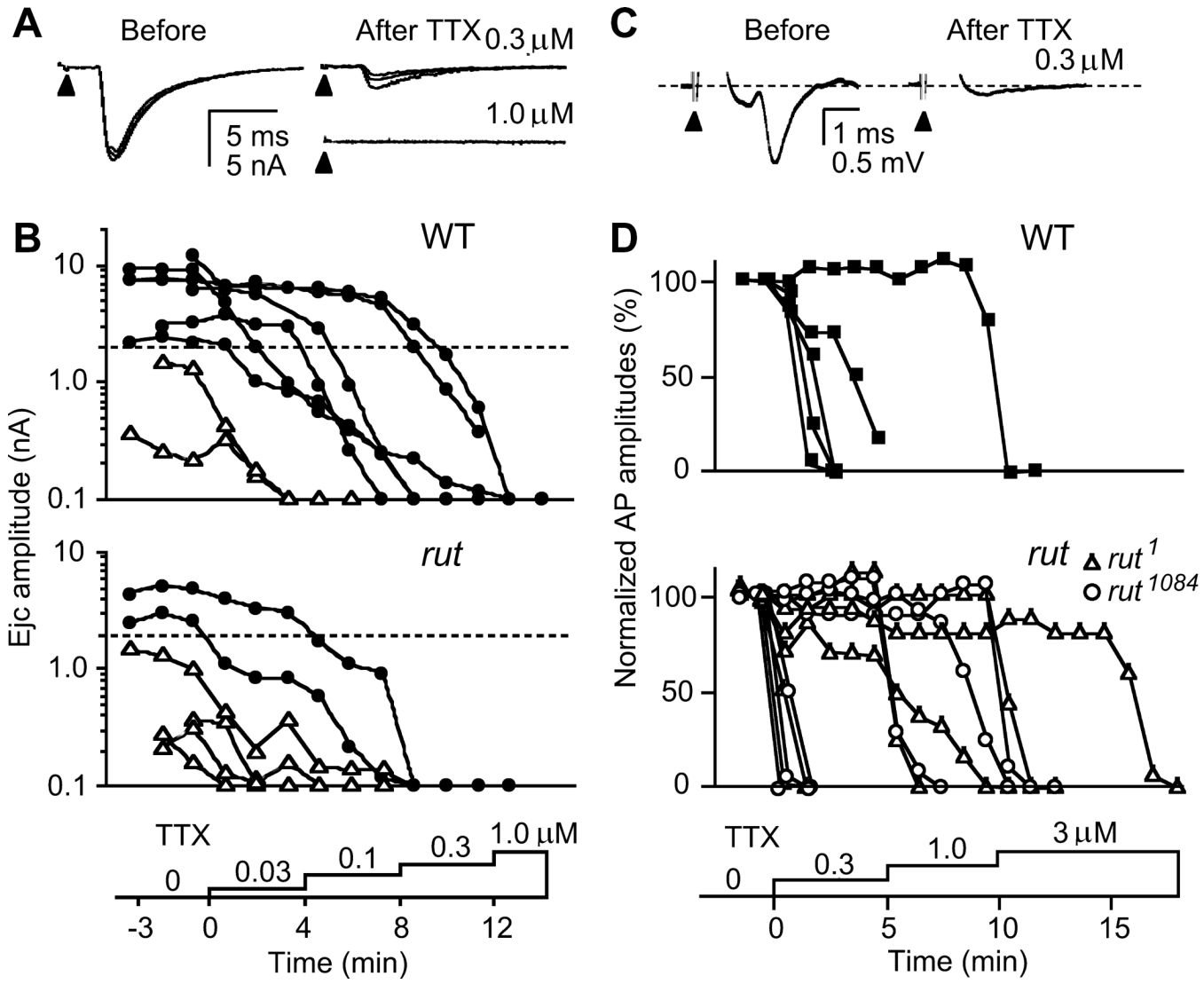

Figure 5.

Sensitivity to TTX paralysis in transmitter release and motor axon action potentials. **A**. Blockade of nerve-evoked ejcs. Focal ejcs were decreased with a low dose (0.3 μM) and abolished with a high dose (1.0 μM) of TTX (three consecutive traces superimposed). **B**. Higher sensitivity to TTX paralysis in *rut* terminals. Ejcs were evoked by 0.1-Hz nerve stimulation while TTX concentrations were increased stepwise (from 0.03 to 1.0 μM). ● and △ indicates ejcs recorded from high- and low-output terminals, respectively. Records from the same bouton were connected with line segments. Note higher TTX sensitivity in low-output terminals. Samples shown reflect the approximate abundance of low-and high-output terminals in *rut* and WT (Figure 1). **C**. TTX blockade of axonal compound action potentials. Action potentials were recorded en passant with a suction electrode from the segmental nerve that contains motor axons innervating larval body wall muscles while TTX was applied stepwise at increasing concentrations. Sample traces from WT nerve show compound action potential before and after TTX blockade. **D**. Overlapping ranges of TTX concentration for action potential blockade of WT and *rut* motor axons. No significant difference was found between WT and *rut* alleles in 50 % blockade concentrations ($p > 0.05$, t-test).

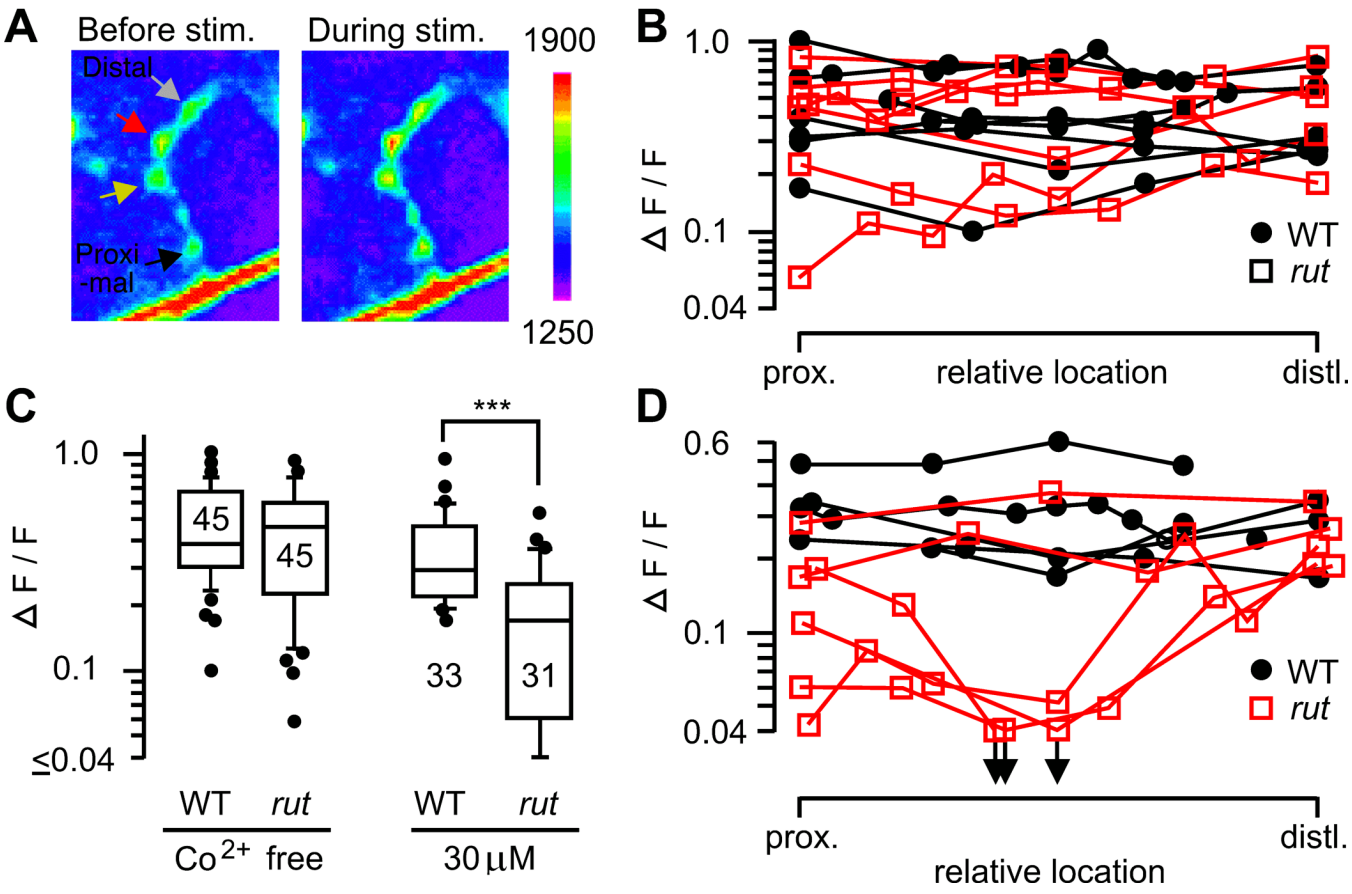

Figure 6.

Uniformity of Ca^{2+} channel-dependent Ca^{2+} accumulation in motor terminal branches. **A**. Presynaptic Ca^{2+} accumulation was monitored with a Ca^{2+}-sensitive green fluorescent protein, GCaMP, expressed in motoneurons (see Methods). Fluorescence intensities in WT presynaptic boutons before and during nerve stimulation (20 Hz, 5 s) are shown. **B**. Ca^{2+} accumulation along motor terminals in WT and *rut*. Note uniform amplitudes of ΔF/F within individual nerve terminals. **C**. Increased sensitivity of rut^1 terminals to a Ca^{2+} channel blocker, Co^{2+}. Peak ΔF/F during 20-Hz stimulation was significantly reduced by 30 μM Co^{2+} in *rut* but not in WT terminals (***, $p < 0.001$; t-test). **D**. Increased variation among *rut* terminals after partial Co^{2+} blockade (30 μM). The symbols in **B** and **D** represent the relative positions of individual boutons along the type Is terminal. Boutons along individual WT (filled circles) and *rut* (open squares) terminals are connected with line segments.

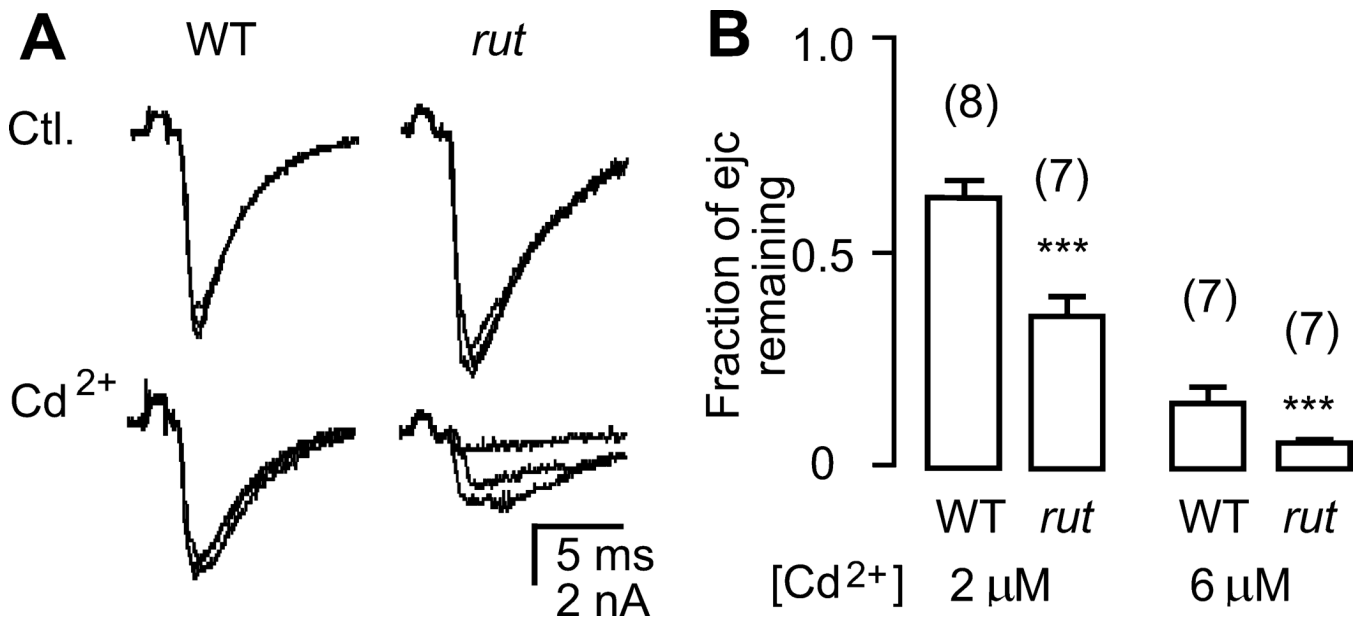

Figure 7.

Increased sensitivity of transmitter release from *rut* terminals to the Ca^{2+} channel blocker Cd^{2+}. **A**. More sever suppression of electrotonically induced ejcs in *rut* terminals by Cd^{2+} (2 µM) in the presence of TTX (3 µM). **B**. Pooled data demonstrating significantly smaller ejcs remaining in *rut* terminals after application of 2 and 6 µM Cd^{2+}. ***, $p < 0.001$; t-test. Mean, SEM, and the number of recording sites (one per larva) are indicated.

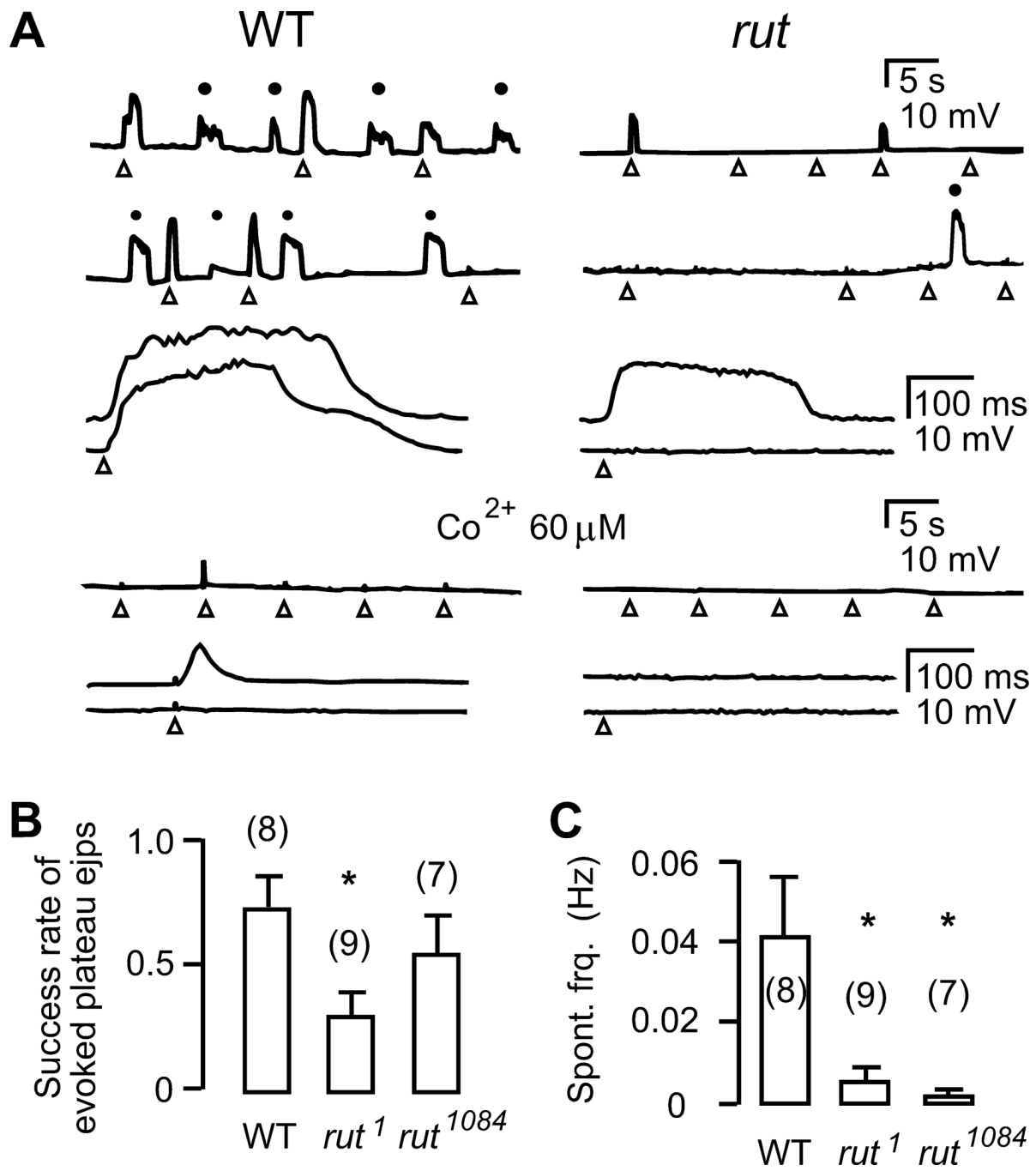

Figure 8.

Ca^{2+}-dependent axon terminal excitability. **A**. Spontaneous (●) and electrotonically evoked (△) long-lasting plateau ejps recorded intracellularly in the presence of Na^+ and K^+ channel blockers (3 µM TTX, 200 µM 4-AP, 20 µM TEA, and 100 µM quinidine in HL3.1 saline containing 0.1 mM Ca^{2+}, see Methods). Evoked plteau ejps are also displayed with a faster time scale in lower traces. Plateau ejps, observed only after inhibiting K^+ channel function, reflect transmitter release caused by prolonged presynaptic depolarization (see text). Occurrence of both spontaneous and evoked plateau ejps was decreased in *rut*. These plateau ejps were suppressed by the Ca^{2+} channel blocker Co^{2+} (60 µM). **B**. Reduced probability of

evoking plateau ejps by electrotonic stimulation in *rut*^{1}. **C**. Reduced frequency of spontaneously occurring plateau ejps in two *rut* alleles. Spontaneous plateau ejps varied in amplitude and only those with amplitude ≥ 20 % of maximally attainable plateau ejps in the same branch were included in the samples. *, $p < 0.05$; t-test. Mean and SEM from the number of terminals examined are indicated.

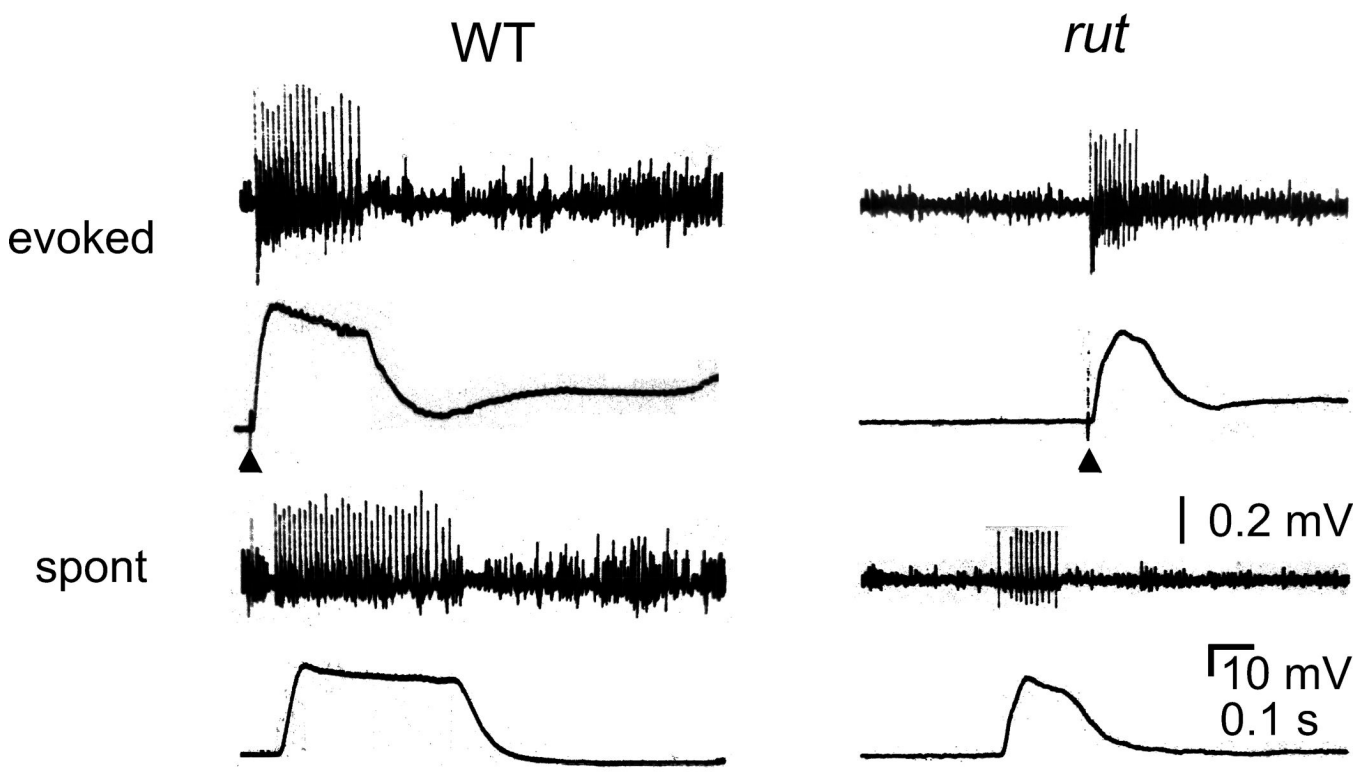

Figure 9.

Simultaneous recordings of plateau ejps and motor axon repetitive firing. Plateau ejps similar to those in Figure 8 were recorded in HL3.1 saline containing 0.1 mM Ca^{2+} and K^{+} channel blockers (200 μM -AP and 20 mM TEA). Without TTX treatment, Na^{+} action potentials were unimpaired and repetitive firing of motor axon accompanied plateau ejps, either evoked by a single nerve stimulus (arrow head) or occurring spontaneously. The interaction between Na^{+} and Ca^{2+} currents in motor axon terminals is revealed by these supernumerary spikes, which propagated antidromically and were sensitive to low doses of TTX and Co^{2+} (see text. c.f. Ganetzky & Wu, 1982;Ueda & Wu, 2006).